We are IntechOpen, the world's leading publisher of Open Access books Built by scientists, for scientists

6,900
Open access books available

185,000
International authors and editors

200M
Downloads

Our authors are among the

154
Countries delivered to

TOP 1%
most cited scientists

12.2%
Contributors from top 500 universities



WEB OF SCIENCE™

Selection of our books indexed in the Book Citation Index in Web of Science™ Core Collection (BKCI)

Interested in publishing with us?
Contact book.department@intechopen.com

Numbers displayed above are based on latest data collected.
For more information visit www.intechopen.com



8

Spatial and Temporal Variability of Sea Surface Temperature in the Yellow Sea and East China Sea over the Past 141 Years

Daji Huang[1,2], Xiaobo Ni[1], Qisheng Tang[3], Xiaohua Zhu[1,2] and Dongfeng Xu[1,2]
[1]*State Key Laboratory of Satellite Ocean Environment Dynamics Second Institute of Oceanography, State Oceanic Administration*
[2]*Department of Ocean Science and Engineering, Zhejiang University*
[3]*Yellow Sea Fisheries Research Institute, Chinese Academy of Fishery Sciences China*

1. Introduction

The Yellow Sea and East China Sea (YES) are marginal seas in the northwest Pacific. There is in fact a smaller sea, the Bohai Sea, to the north of the Yellow Sea. For most discussions in the chapter, we shall treat the Bohai Sea as part of the Yellow Sea. The YES is one of the mostly intensively utilized sea in the world, for example, heavy fishery and marine aquaculture. The use of the YES is closely related to its climate variability, though it is not well-know because until now there has been a lack of adequate observational data. To know the climatology of sea surface temperature (SST, all the acronyms used in the chapter are listed in Table 1) in the YES and their relationship with regional and global climate have both scientific and social importance.

There have been recent studies, some associated with marine ecosystem, on the long-term temperature variation in the YES. The results indicate that SST has risen significantly in the 20th century. The observed annual mean SST in the Bohai Sea increased by 0.42℃ from 1960 to 1997 (Lin et al., 2001), and the observed annual mean of water-column average temperature along the 36°N section between 120°45′E and 124°30′E in the Yellow Sea increased by 1.7℃ from 1976 to 2000 (Lin et al., 2005). On the eastern side of the Yellow Sea, there has been an increase of 1.8℃ and 1.0℃, respectively, in water temperature in February and August over the past 100 years (Hahn, 1994). Using the Hadley SST data from 1901 to 2004, Zhang et al. (2005) found that, in the YES, the annual mean SST was cold from 1900s to 1930s, warm in the 1950s, slightly cold in the 1960s and warming again from 1980s.

Until now, the inter-relation between the SST in the YES with the regional climate is not well documented, though their interaction is rather distinct, for instance, the variability of the land surface air temperature over China affects the SST in the YES particularly in winter, and the SST in the YES also have some influence on the air temperature, fog and precipitation over China, especially along the coastal area. However these have not been well studied, especially in climatological prespective due to the lack of long time dataset.

For all study of the spatial and temporal variability of SST in the YES, the annual mean data is used, while seasonal variability is filtered out. In this study, we use the Met Office Centre's Hadley SST data (Rayner et al., 2003) to investigate the seasonal variability, inter-annual to decadal variability and long-term trend of SST in the YES.

Acronym	Expanded form
AC	annual component
AM	annual mean component
AR	annual range
CC	cold regime with a cold trend,
CW	cold regime with warm trend
EASM	the East Asian summer monsoon
EMD	Empirical Mode Decomposition
ENSO	El Nino–Southern Oscillation
EOF	Empirical Orthogonal Function
JJA	June, July and August
JMA	the Japan Meteorological Agency
PAC	the normalized annual precipitation anomaly over China
PDO	Pacific Decadal Oscillation
RMSE	root mean squared error
STD	standard deviation
SST	sea surface temperature
TAC	annual surface air temperature anomaly over China
WC	warm regime with cold trend
WW	warm regime with warm trend
YES	the Yellow Sea and East China Sea

Table 1. List of the acronyms used in the chapter

2. Data and methods

2.1 Data

The monthly SST in the YES is extracted from HadISST1 SST dataset for the period from 1870 to 2010, i.e., 141 years. There are 188 grid points in the YES (Fig. 1). HadISST1 SST data set, produced by the Met Office Hadley Centre, is a monthly global 1° latitude-longitude grid data start from 1870 till present. HadISST1 temperatures are reconstructed using a two-stage reduced-space optimal interpolation procedure, followed by superposition of quality-improved gridded observations onto the reconstructions to restore local detail. HadISST1 compares well with other published analyses, capturing trends in global, hemispheric, and regional SST well, containing SST fields with more uniform variance through time and better month-to-month persistence than those in global SST (Rayner et al., 2003). HadISST1 SST dataset is available at web site http://www.metoffice.gov.uk/hadobs/hadisst/data/download.html.

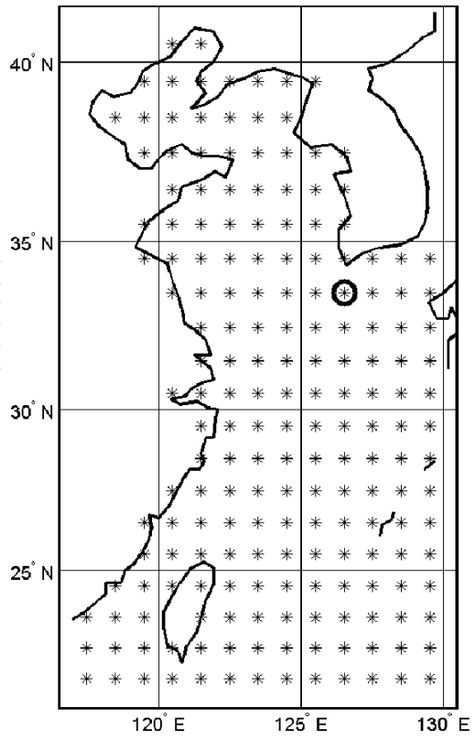


Fig. 1. Study area of the YES, and location of data grid points extracted from HadSST1 SST dataset. A bold cycle indicates the specific data points at (126.5°E, 33.5°N), which is used as a template.

The spatial and temporal variability of SST in the YES is related to the regional and global climate. One climatic effect of the SST in the YES is readily illustrated by much warmer winter temperatures on its east coast than that on the west coast. For example, January temperature is 6.4°C in Nagasaki (32.4°N), Japan, but only 3.7°C in Shanghai (31.3°N), China (Xie et al., 2002). Both the satellite observation and numerical model results show (Xie et al., 2002; Chen et al., 2003) that SST front in the YES plays a significant role on enhancing wind speed and raining cloud above the region. The SST in the YES (a marginal sea between the largest continent Eurasia and the largest ocean Pacific) is a part of the global climate and is closely linked to the Pacific and East Asian climate. The East Asian monsoon system is one of the most active components of the global climate system. El Nino–Southern Oscillation (ENSO) exhibits the greatest influence on the interannual variability of the global climate (Webster et al., 1998). The mature phase of ENSO often occurs in boreal winter and is normally accompanied by a weaker than normal winter monsoon along the East Asian coast (Wang et al., 2000). Consequently, the climate in south-eastern China and Korea is warmer and wetter than normal during ENSO winter and the following spring (Tao & Zhang, 1998; Kang & Jeong, 1996).

In order to investigate the relationship of the variability of SST in the YES with the regional and global climate, the following time series are used.

The annual surface air temperature anomaly over China (TAC), the normalized annual precipitation anomaly over China (PAC) and the East Asian summer monsoon (EASM) index are used to represent the regional climate. The TAC is reconstructed by Tang & Ren

(2005) for 1905 to 2001 and extended by Ding & Ren (2008) to 2005. A monthly mean temperature data obtained by averaging monthly mean maximum and minimum temperatures is used to avoid the inhomogeneity problems with data induced by different observation times and statistic methods between early and late 20th century. The PAC is reconstructed by Ding & Ren (2008), and is normalized with respect to its 30 years (1971-2000) standard deviation (STD). Both TAC and PAC are available from 1905 to 2005 and these time series are digitalized from their published figures (Ding & Ren, 2008).

The EASM index is defined as an area-averaged seasonally (June, July and August, JJA) dynamical normalized seasonality at 850 hPa within the East Asian monsoon domain (10°N-40°N, 110°E-140°E) (Li & Zeng, 2003). There is an apparent negative correlation between the EASM index and summer (JJA) rainfall in the middle and lower reaches of the Yangtze River in China, indicating drought years over the valley are associated with the strong EASM and flood years with the weak EASM. The annual ESAM index is available from 1948 to 2010 and is downloaded from http://web.lasg.ac.cn/staff/ljp/data-monsoon/EASMI.htm.

Both ENSO and Pacific Decadal Oscillation (PDO) indexes are used to represent the global climate. The ENSO index used in the chapter is produced by the Japan Meteorological Agency (JMA). It is the monthly SST anomalies averaged for the area 4°N-4°S and 150°W-90°W. This ENSO index is the JMA index based on reconstructed monthly mean SST fields for the period Jan 1868 to Feb 1949, and on observed JMA SST index for March 1949 to present (Meyers et al., 1999). The monthly ENSO index data file (jmasst1868-today.filter-5) is available from 1868 to 2010 and is downloaded from http://coaps.fsu.edu/pub/JMA_SST_Index/.

The PDO index used in the chapter is updated standardized values for the PDO index, derived as the leading principal component of monthly SST anomalies in the North Pacific Ocean, poleward of 20°N (Zhang, et al., 1997; Mantua et al., 1997). The monthly mean global average SST anomalies are removed to separate this pattern of variability from any "global warming" signal that may be present in the data. The monthly PDO index is available from 1900 to present and is downloaded from http://jisao.washington.edu/pdo/PDO.latest.

All the above mentioned five time series are shown in Fig. 2.

2.2 Data analysis methods

The monthly SST of the last 141 years in the YES contains both spatial and temporal variability. The temporal variability is primarily contributed by seasonal signal for overall variability, and is contributed by inter-annual to decadal signals for the annual mean variability. For long-term variability analysis, it is a common way to remove seasonal signal, and explore only on low frequency variability, i.e., inter-annual to decadal scales and long-term trend. Here, in addition to the common way for analyzing low frequency variability, we shall also investigate seasonal signal to know its spatial and temporal variability. Hereafter, we shall use the term “annual component” (AC) instead of seasonal signal, and “annual mean component” (AM) instead of inter-annual to decadal scales and long-term signal.

The AC as well as AM is spatially interrelated with specific spatial patterns. We shall firstly separate AC and AM from the monthly SST at each grid point. Then, the pattern recognition is used for AC to identify the normalized annual pattern and the time-dependent annual range (AR). The normalized annual pattern is fitted with annual and semi-annual sinusoidal functions to get their amplitudes and time lags. Both AR and AM are further analyzed with

Empirical Orthogonal Function (EOF) methods (Emery & Thomson, 2001) to explore their spatial and temporal variability.

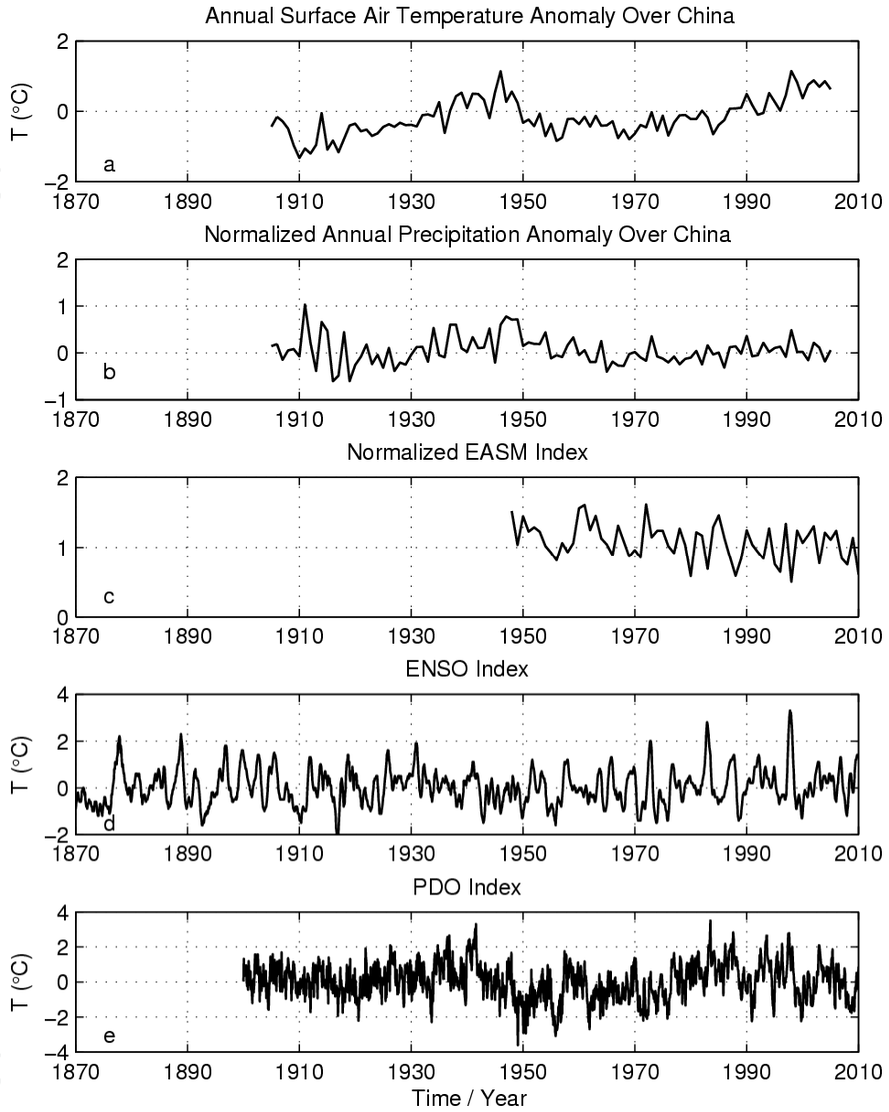


Fig. 2. Time series used to represent regional and global climate. a) Annual surface air temperature anomaly over China (TAC). b) Normalized annual precipitation anomaly over China (PAC). c) EASM Index. d) ENSO index. e) PDO index.

2.2.1 Partition SST into AC and AM

The SST at each grid point is partitioned into AC and AM by applying twice a 12 points moving average on the SST, namely, AM is obtained by moving average and AC is derived by subtracting AM from the SST. For instance, the SST at a specific location (126.5°E, 33.5°N), and the partitioned AC and AM are shown in Fig. 3. The much larger AR of AC for 17℃ than the range of AM for 3℃means that seasonal variability is much stronger than low frequency variability on inter-annual to decadal scales.

2.2.2 Harmonic analysis of AC

Fig. 3b shows that AC neither is a sinusoidal function, nor has time independent amplitude. The great similarity of AC suggests that AC at each grid point can be expressed with an annual pattern, especially with a normalized annual pattern, multiply by a time varying AR.

$$SST_{AC} = \frac{1}{2} AR * T_{Norm} \quad (1)$$

Where SST_{AC} is AC of SST at a grid point, T_{Norm} is annual pattern of AC normalized by half AR. T_{Norm} is further fitted with annual and semi-annual sinusoidal harmonic functions, which are expressed by their amplitudes and time lags as follows.

$$T_{Norm} = h_1 \cos[\frac{2\pi}{12}(t-t_1)] + h_2 \cos[\frac{4\pi}{12}(t-t_2)] + \Delta T \quad (2)$$

Where, t is time in month and increases from 1 to 12 for January to December. h_1 and h_2 are amplitudes of the annual and semi-annual harmonic functions. t_1 and t_2 are time lags in month of the annual and semi-annual harmonic functions.

Fig. 4 shows the AC of SST at a specific location (126.5°E, 33.5°N) and the validation of above expressions (1) and (2). Fig. 4a and Fig. 4c demonstrate that AC has similar annual pattern with maximum and minimum SST in August and February. The annual maximum and minimum SSTs vary very significantly from year to year, and their temporal variability is reflected by AR (Fig. 4b). The much reduced dispersion and deviation of normalized annual pattern in Fig. 4d mean that normalized annual pattern is a better representation than the un-normalized annual pattern for pattern recognition. The derived annual and semi-annual harmonic functions, namely c_1 and c_2, are shown in Fig. 4e. The small difference (ΔT) between the SST pattern and sum of annual and semi-annual harmonic functions (c_1+c_2) suggests that annual pattern can well be described by equation (2).

2.2.3 Analysis of AR and AM

The time varying AR and AM are further analyzed with EOF method. Firstly, both AR and AM are partitioned into their time independent mean and time dependent anomaly expressed statistically by STD (Fig. 6, Fig. 8). Then, their anomalies are analyzed with EOF method, by decomposing their spatial-temporal anomaly to coherent spatial modes and corresponding temporal modes (Fig. 7, Fig. 9). The larger variance explained by the first two leading EOF modes in general, and the dominant contribution of the first mode in particular, means that the spatial and temporal variability of AR and AM can well be described by their first EOF mode. Conventionally, the spatial mode is normalized to be a unit vector, and the magnitude of variability is expressed in the corresponding temporal mode. This expression is more mathematical than physical, as it is hard to extract the actual variability at a specific time and place by combine the spatial and temporal value. In present chapter, we shall normalize the temporal mode by its maximum, and the magnitude of variability is reflected by the corresponding spatial mode. And the spatial mode is actually the maximum variability occurred when the temporal mode equals one. In this way, we can easily estimate the actual variability at a specific time and place, just by multiply the spatial mode values at that place by the temporal mode value at that time.

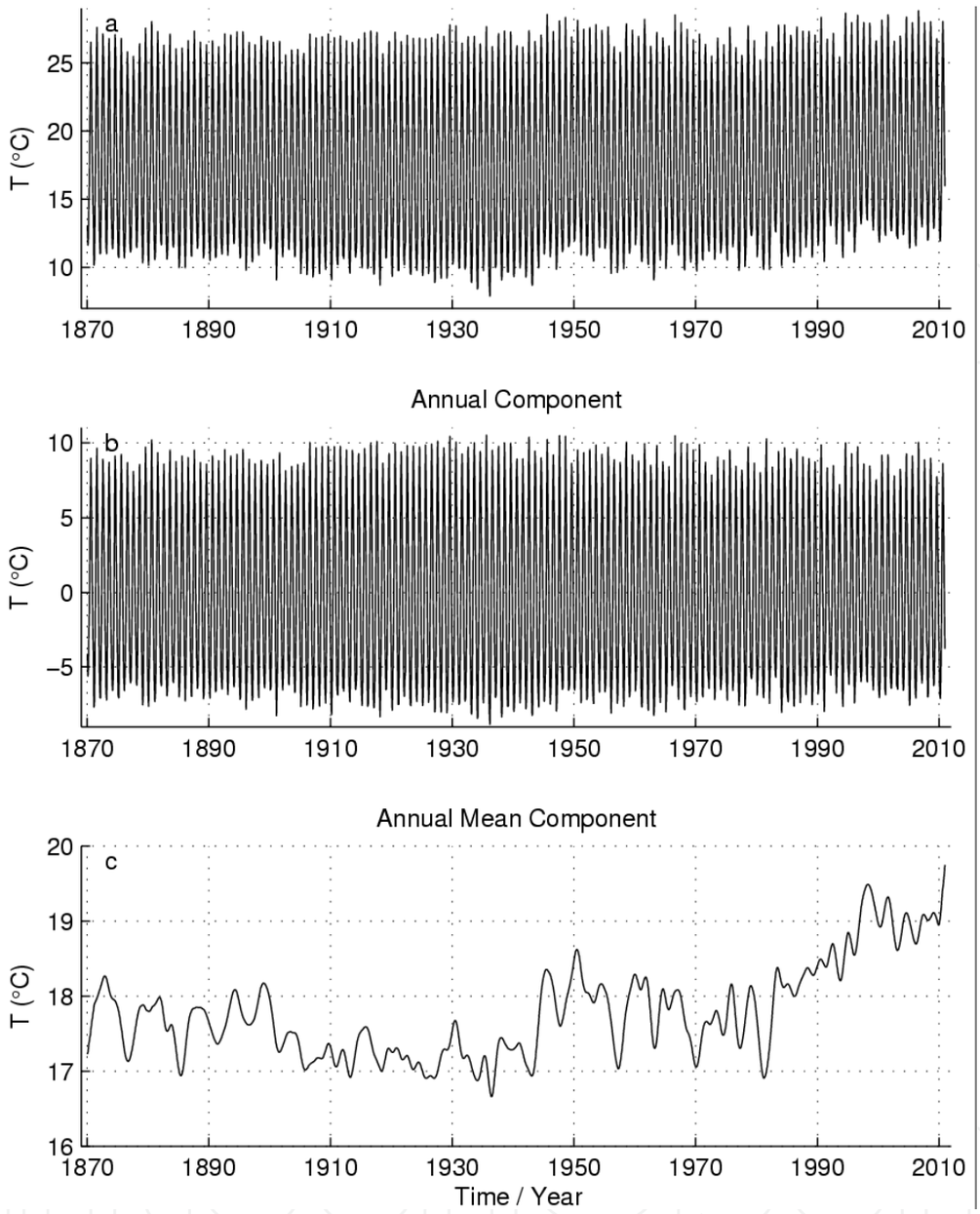


Fig. 3. Partition of SST into AC and AM. a) SST at specific location (126.5°E, 33.5°N) as indicated by a bold circle in Fig. 1. b) Decomposed AC with zero annual mean. c) Derived low frequency de-annual component, AM.

2.2.4 Analysis of regime shifts

The first temporal EOF mode of AM is further analyzed with Empirical Mode Decomposition (EMD) methods (Huang et al., 1998; Huang et al., 2003; Huang et al., 2008). Regime shifts are identified by the decomposed components (Fig. 10). The increase of SST over the latest regime, namely from 1977 to 2010, is fitted with linear regression to obtain the degree of warming of SST in the YES (Fig. 11).

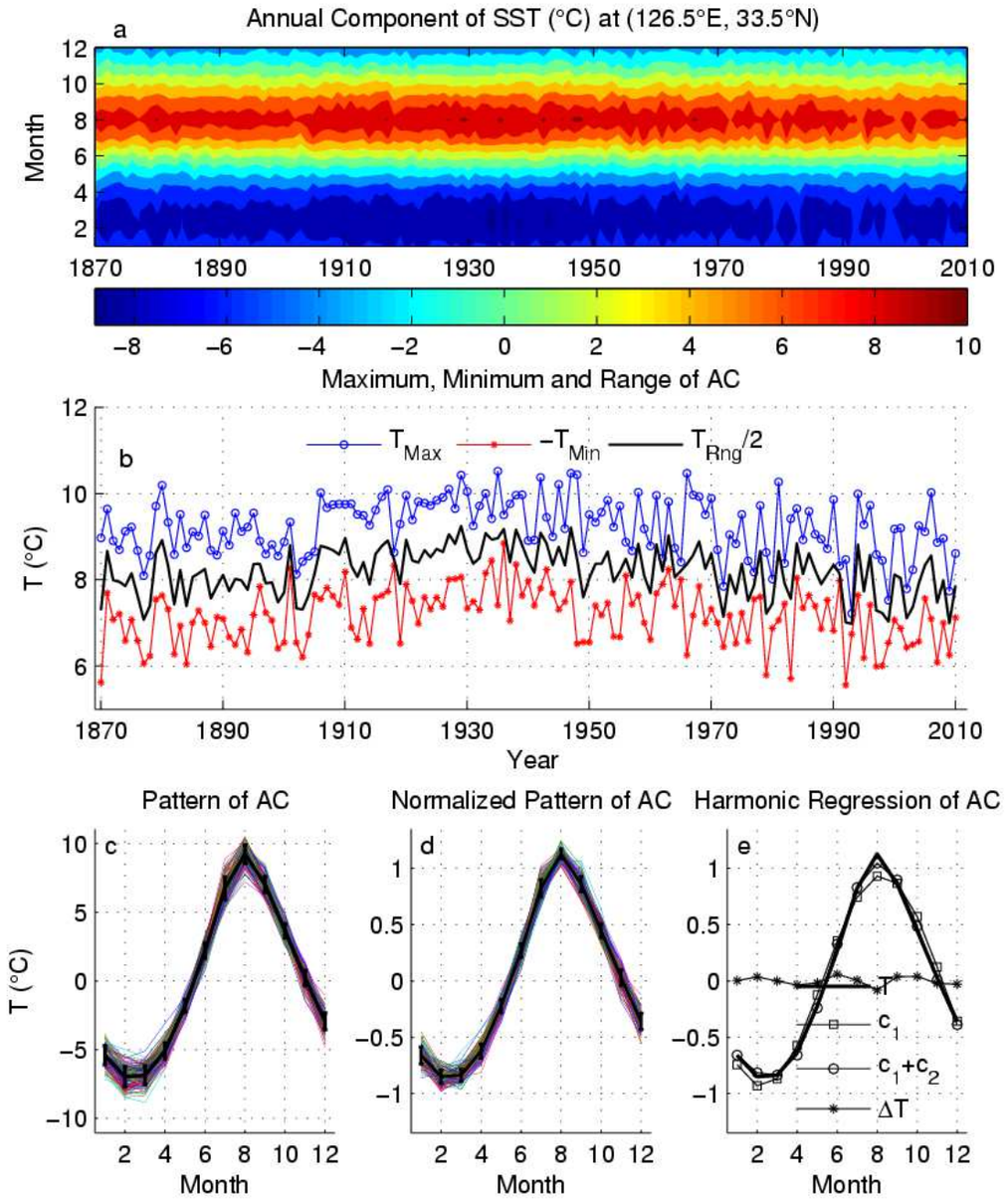


Fig. 4. AC of SST at a specific location (126.5°E, 33.5°N). a) Its contour map. b) The maximum, minimum and half range of AC. c) Annual pattern for 141 years. d) Annual pattern normalized by half AR. e) Harmonic regression of mean normalized annual pattern with annual and semi-annual sinusoidal functions, c_1 and c_2. ΔT is the difference between T and their sum c_1+c_2.

3. Results

We shall present the obtained results from high frequency to low frequency. The spatial and temporal variability of AC will be presented first in terms of normalized annual pattern and AR, followed by AM. The regime shift of AM is presented in conjunction with AR. Finally, we present the correlation between AR and AM with regional and global climate.

3.1 Normalized annual pattern

The fitting of the mean normalized annual pattern with annual and semi-annual sinusoidal functions is validated by root mean squared error (RMSE), which is shown in Fig. 5f. The RMSE is less than 0.04℃ in general, comparing with the range of mean normalized annual pattern of 2℃, which means that the mean normalized annual pattern can well be represented by annual and semi-annual sinusoidal functions.

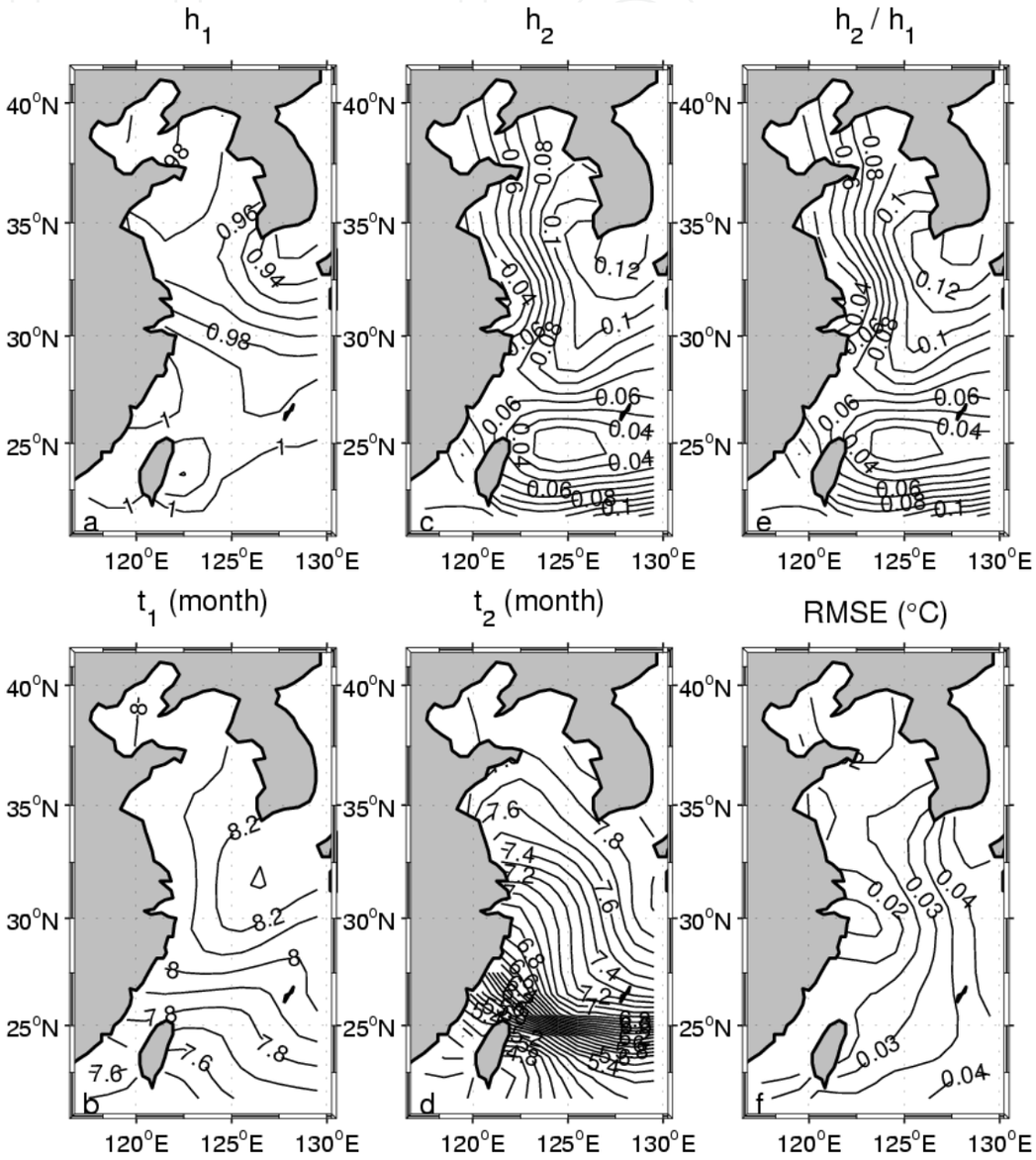


Fig. 5. Harmonic regression of the mean normalized annual pattern with sinusoidal functions. a) h_1, amplitude of annual sinusoidal component. b) t_1, time lag of annual sinusoidal component. c) h_2, amplitude of semi-annual sinusoidal component. d) t_2, time lag of semi-annual sinusoidal component. e) h_1/h_2, ratio of the amplitude of semi-annual to annual components. f) RMSE of harmonic regression of the mean normalized annual pattern with annual and semi-annual sinusoidal functions.

The annual and semi-annual sinusoidal functions are described simply by their harmonic constants, i.e., amplitudes and time lags. The large and close to 1 amplitude (h_1>0.94℃, Fig. 5a) of annual sinusoidal function means that normalized annual pattern is over dominant by pure annual cycle. The small amplitude of semi-annual sinusoidal function (h_2<0.12℃, Fig. 5c) means that annual cycle is modified by semi-annual fluctuation, which is most significant to the south of Korean Peninsula. The small ratio of h_2/h_1 (Fig. 5e), which has a very similar spatial pattern to h_2 due to nearly one value of h_1, confirms that annual cycle is much more important than semi-annual cycle.

The time lag of the annual cycle, t_1, is shown in Fig. 5b. From Fig. 5b, the maximum annual SST occurs in later July in the south of YES, and delays gradually northward by half a month to early August in the central YES. In the north part of YES, the maximum annual SST occurs at the beginning of August. Fig. 5d shows that time lag of the semi-annual cycle, t_2, which means that the first maximum semi-annual SST occurs in later April in the southern YES, and delays rapidly north-eastward by three months to later July in the central YES. The semi-annual cycle plays a primary modification on annual cycle, particularly in the area south to Korean Peninsula, where h_2 is largest. The effects of this modification lead to a warmer SST in August and February, which can be clearly identified from Fig. 4e.

3.2 Spatial and temporal variability of AR

Fig. 6a and 6b show the mean and STD of AR. The mean AR increases from 6℃ in south to 24℃ in the Bohai Sea. The lower AR in the southern YES means that SST has less annual variability, and the higher AR in the northern YES means that SST has larger annual

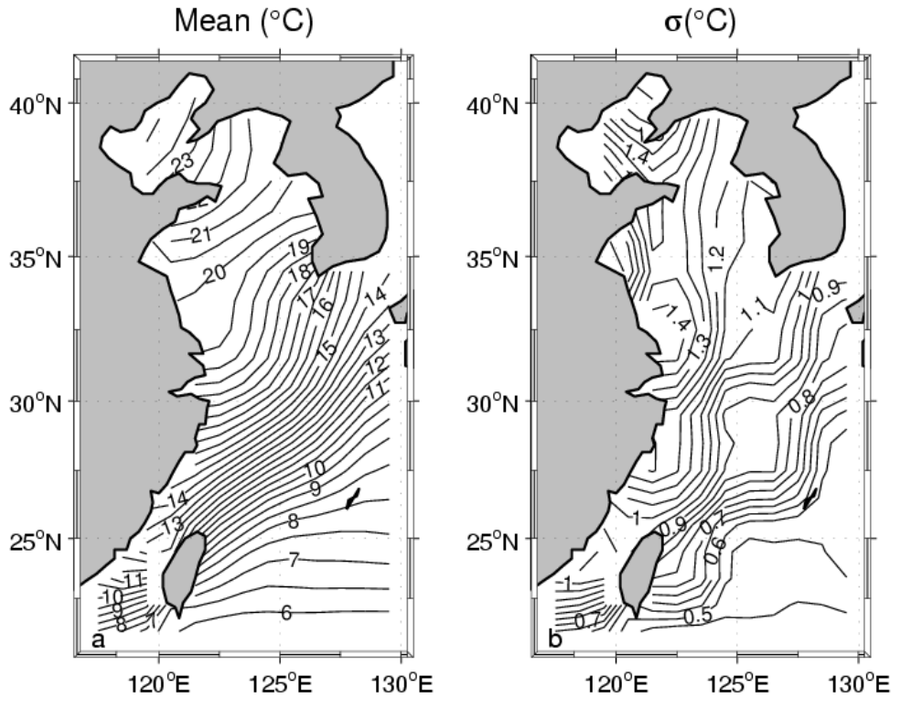


Fig. 6. Mean and STD of AR. a) mean. b) STD.

variability. There is a band of rapid change of mean AR in the continental margin of YES, where, the mean AR increases from 9℃ in the southeast YES to 19℃ in the central Yellow Sea. This band marks a transition zone between oceanic to continental dominant climate.

The STD of AR shows a similar spatial tendency as its mean, i.e., STD increases from 0.5℃ in south to 1.6℃ in the Bohai Sea. There is a band of relatively larger STD oriented primarily in south-north direction in the western YES. Corresponding to the band of rapid change of mean AR, there is also a zone of rapid change of STD, where STD increases from 0.6℃ in the southeast of YES to 1.2℃ in the central Yellow Sea.

The AR as well as its variability increases from south to north in the YES. Both smaller mean and STD of AR in the south means that SST is much more stationary in the southern YES. While, in the northern Bohai Sea, AR and its variability are very larger, show significant annual variation of SST.

The spatial and temporal variability of AR, as expressed by its variance STD in Fig. 6b, is further investigated with EOF method. The first two leading EOF modes explain 84% of total variance (Fig. 7), and the first mode contributes 69% in particular, mean that the spatial and temporal variability of AR can well be described by the first EOF mode.

The first EOF spatial mode shows a spatially coherent in–phase pattern with its amplitude of less than 1℃ in the south increases to greater than 3℃ in the western YES (Fig. 7a). This spatial pattern is very similar to the spatial pattern of STD, as supported by large contribution of 69%. The corresponding temporal mode shows a very distinct inter-annual to decadal variability (Fig. 7c). The larger positive values of about 0.9 in the temporal mode during 1940s mean that AR is much larger during 1940s, which is about 1℃ larger than mean AR in the southern YES and increases by 3℃ in the western YES (Fig. 7c). AR from 1990 to present is reduced about 0.3℃ in the south to 1℃ in the western YES as indicated by larger negative values of about 0.3 in the temporal mode.

3.3 Spatial and temporal variability of AM

Fig. 8a and 8b show the mean and STD of AM. The mean AM decreases from 26℃ in the south to 13℃ in the north of YES. There is a band of rapid change of mean AM in the continental margin of YES, where, the mean AM decreases from 24℃ in the southeast to 17℃ in the central Yellow Sea. This band coincides with that of AR confirms the transition zone between oceanic to continental dominant climate.

The STD of AM shows a relatively uniform spatial pattern with 0.6℃ over the entire YES, except in the southeast where STD is much reduced due to the oceanic effects and relatively larger STD in the central YES. There is also a zone of rapid change of STD in the southeast YES, but it is shifted from continental margin to Okinawa trench.

The mean AM decreases from south to north, while its variability is almost same in the entire YES. Larger mean AM and small STD in the south means that climatologically mean SST is high and stationary in the southern YES.

The spatial and temporal variability of AM, as expressed by its variance STD shown in Fig. 8b, is further investigated with EOF method. The first two leading EOF modes explain 94% of total variance (Fig. 9), and the first mode contributes 85% in particular, mean that the spatial and temporal variability can well be described by the first EOF mode.

The first EOF spatial mode shows a spatially coherent in-phase pattern with its amplitude of less than 1.2℃ in south increases to greater than 2.0℃ in the central and south-western YES (Fig. 9a). This spatial pattern is very similar to the spatial pattern of STD, as supported by large contribution of 85% to total variance. The corresponding temporal mode shows very distinct inter-annual to decadal variability (Fig. 9c). The larger positive values of about 0.5 in the temporal mode during the last decade mean that AM is much warmer. Particularly in 1998, the AM is warmer than its mean AM about 1.2℃ in south increases to greater than 2.0℃ in the central and south-western YES. Before 1940s, the AM is generally cold than usual, especially in 1920s.

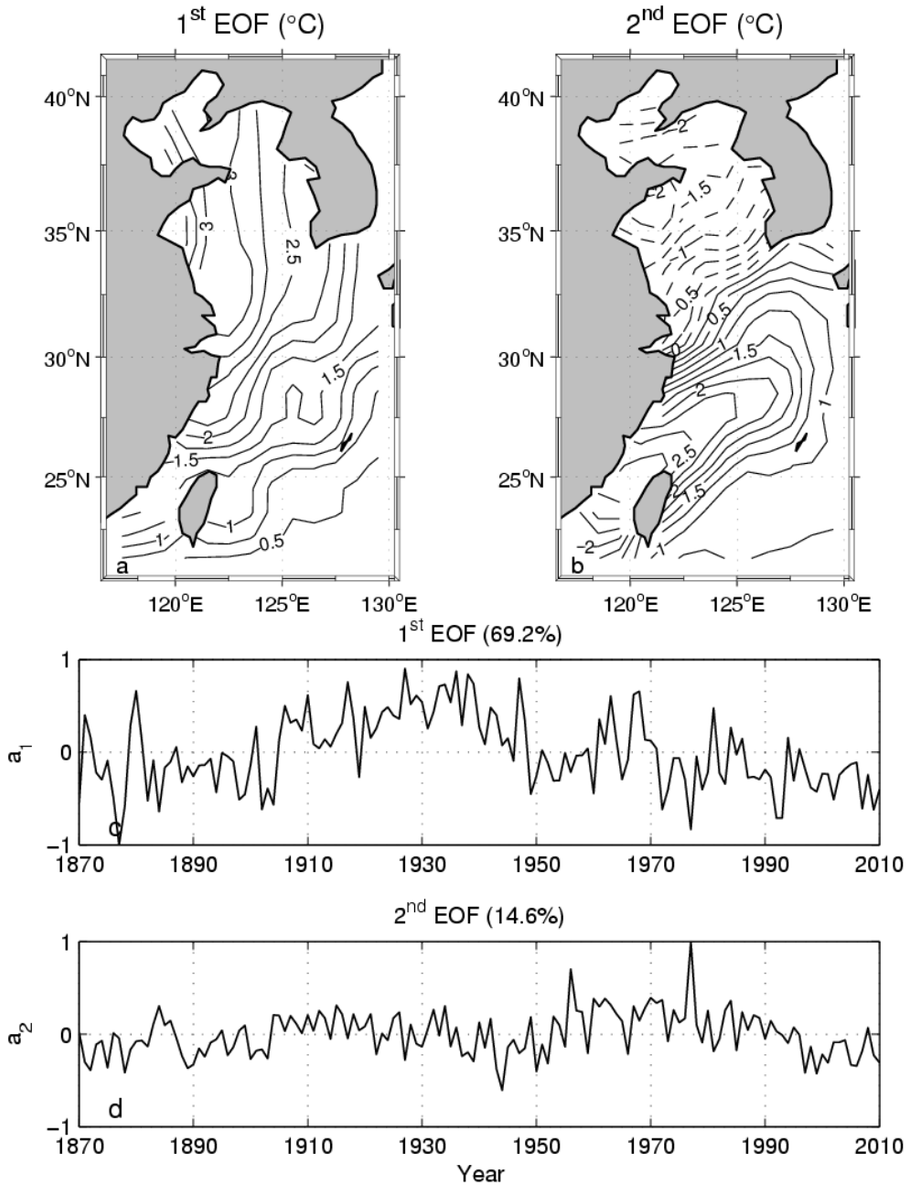


Fig. 7. The spatial and temporal EOF modes of AR. a) The first spatial mode. b) The second spatial mode. c) The first temporal mode. d) The second temporal mode.

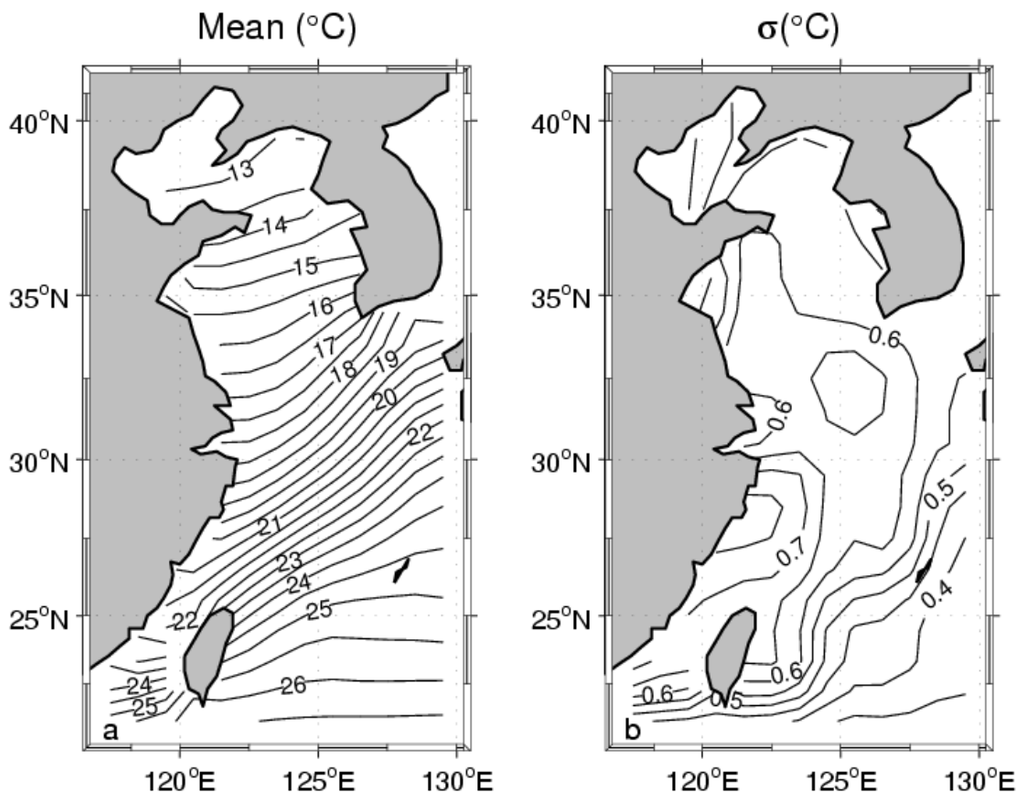


Fig. 8. Mean and STD of AM. a) mean. b) STD.

3.4 Regime shift of AM and AR

Based on EMD analysis of AM and the northern hemisphere air temperature of Asia (Jones & Moberg, 2003), the variability SST in the YES over the last 141 years is classified into four regimes (Fig. 10). Namely, Cold regime with a cooling trend (CC) from 1870 to 1900, the mean SST is a slightly cold than usual and AR reduced by 0.5 STD units. Cold regime with a warming trend (CW) from 1901 to 1944, the mean SST is coldest and is reduced by 1 STD unit than usual mean SST, and AR is largest and is increased by 1 STD unit. The third regime is from 1945 to 1976, which is a warm regime with a cooling trend (WC). The mean SST is slightly warmer than usual and AR is generally in normal. The fourth regime is most obvious; it is a warm regime with a larger warming trend (WW) from 1977 to present. During this warmest regime, AR is reduced about 0.7 STD units with a decrease trend, which means that SST in the YES in getting warmer than ever and with a much reduced annual range. Consequently, the winter SST increase in the YES is significantly amplified than other seasons.

AR and AM are significantly negative correlated as show in Fig. 10c. There are three distinct peaks in the correlation coefficient, with 0, 4 and 10 years time lag of AR with respect to AM. AR lags AM mean that the variability of AM might affect the variability of AR for the lagged time interval. The zero time lag means that, in the year when AM is higher (lower), the corresponding AR is lower (higher) and will have a much warmer (colder) winter SST than usual in the YES.

The warming trend is further explored with its AM by a linear regression at each grid points from 1977 to 2010. The increment of AM from 1977 to 2010 is shown in Fig. 11. The AM has increased from 0.5℃ to the east of Taiwan to more than 1.6℃ in the central YES, especially to 2℃ to the south of Korean Peninsula. The increment of AM is much larger in the mid-shelf than near shelf and Kuroshio regions.

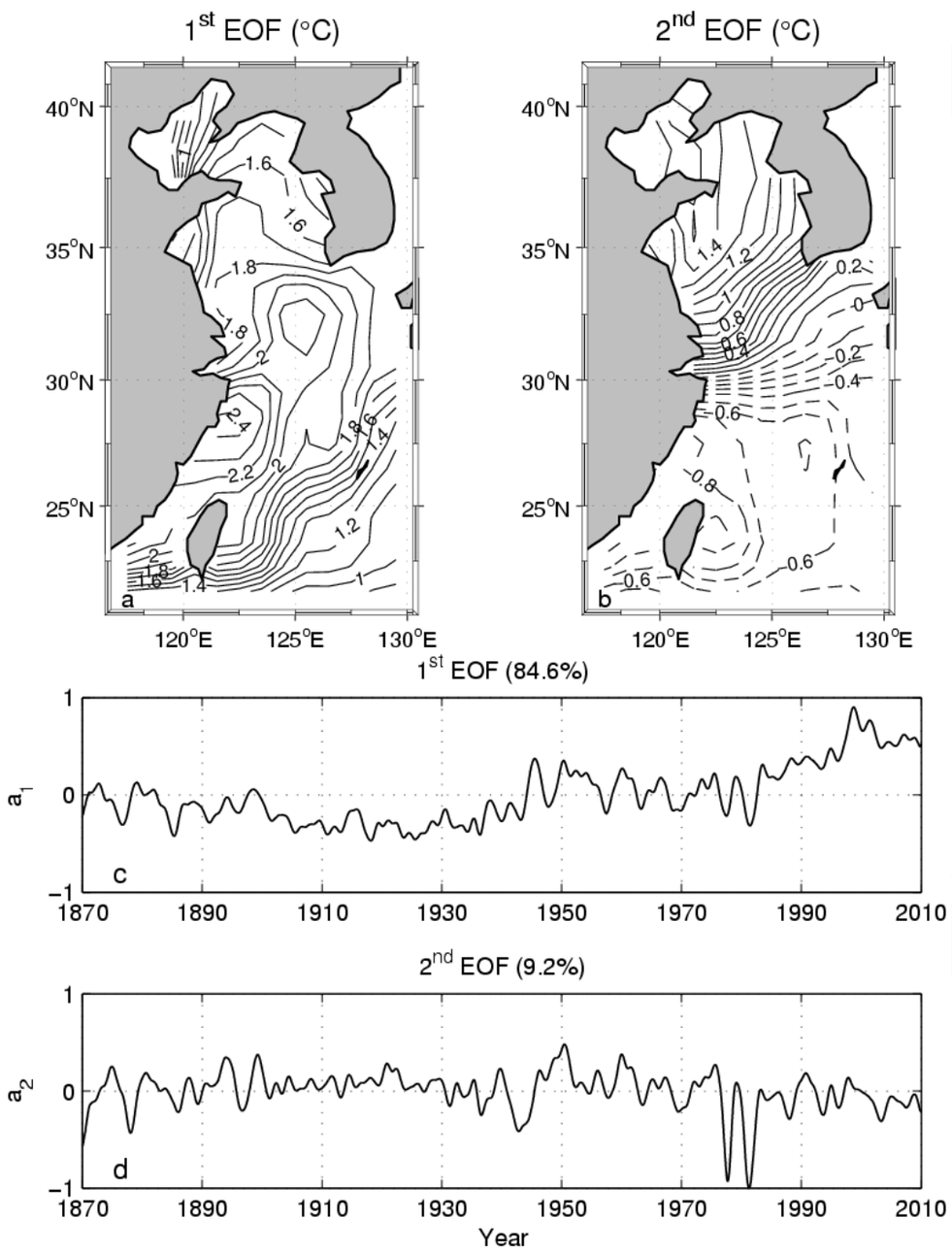


Fig. 9. The spatial and temporal EOF modes of AM. a) The first spatial mode. b) The second spatial mode. c) The first temporal mode. d) The second temporal mode.

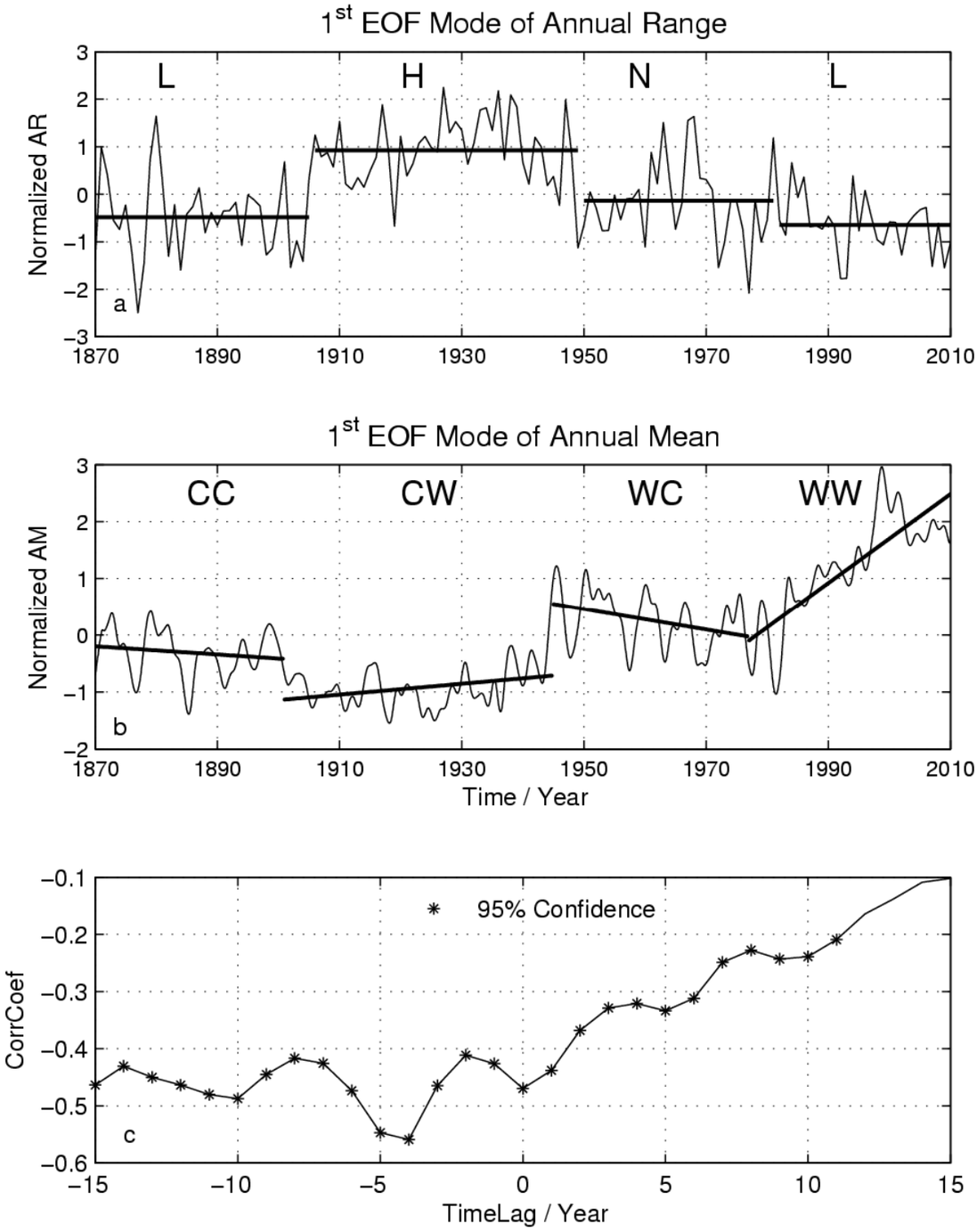


Fig. 10. The regime shifts of SST in the YES. a) The four regimes of in the first EOF mode of AR, L, H and N stand for the low, high and normal variability of AR. b) The four regimes of the first EOF mode of AM, CC, CW, WC and WW stand for the cold regime with a cold trend, cold regime with warm trend, warm regime with cold trend and warm regime with warm trend. c) Correlation coefficient between AR and AM, negative (positive) time lag means that AR lags (leads) AM.

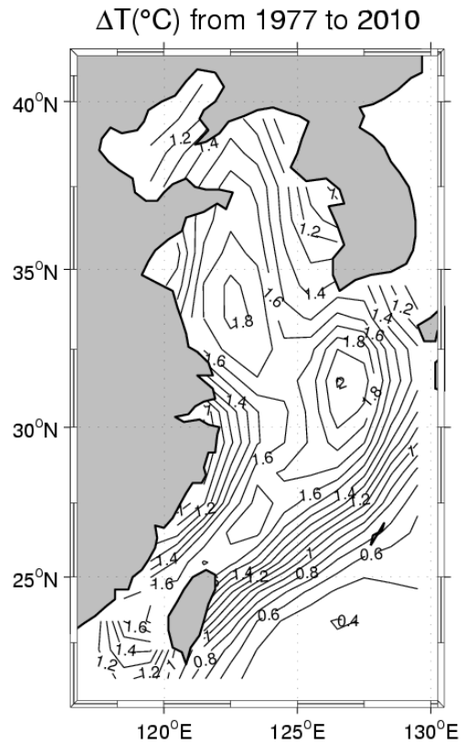


Fig. 11. The increment of AM in the YES over the latest warm regime from 1977 to 2010.

3.5 Relationship between AR and regional and global climate

The variability of AR and AM are closely related to regional and global climate. Their relationships are explored with the correlation between the first EOF temporal mode of AR and AM with TAC, PAC and EASM index which represent regional climate, and with ENSO and PDO indexes which represent global climate.

The time lagged correlation coefficients between the first EOF temporal mode of AR with TAC, PAC, EASM index, ENSO index, and PDO index are shown in the left column of Fig. 12 from top to bottom.

AR is significantly correlated with regional climate, as shown in Figs. 12a to 12c. The peak in Fig. 12a shows that AR and TAC are significantly (95% confidence interval, same hereafter) negative correlated with correlation coefficient of -0.5 for a 10a time ahead for AR against TAC. This correlation coefficient suggests that AR is significantly related with the regional land air temperature anomaly, larger (smaller) AR corresponds to negative (positive) TAC, and the larger AR is generally related to the colder surface air temperature over China 10 years later.

AR and PAC are significantly positive correlated with correlation coefficient of 0.35 for 12a ahead for PAC against AR. AR and EASM index are significantly positive correlated with correlation coefficient of 0.34 for zero time lag, 0.32 for 5a time ahead, 0.33 for 15a time ahead, and 0.32 for 23a time ahead for EASM against AR. As shown in Fig. 12c, strong EASM is generally related to a higher AR of SST in the YES for the corresponding year, 5a, 15a and 23a later.

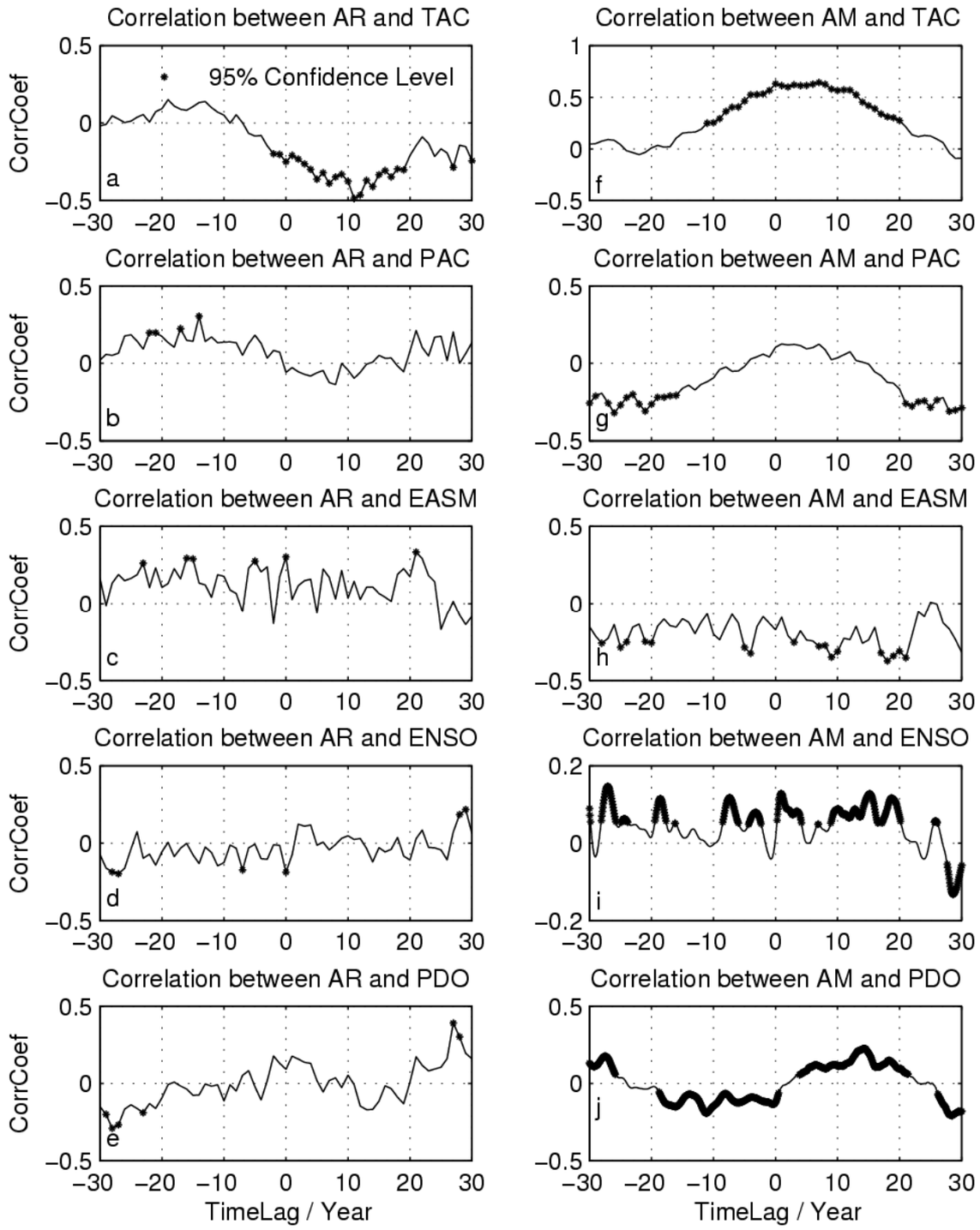


Fig. 12. Relationship between AR and AM with TAC, PAC, and EASM, ENSO and PDO indexes from left to right and top to bottom. Star on line indicates that the corresponding correlation is significant on 95% confidence interval.

AR is also significantly related to the global climate, as shown in Fig. 12d and 12e. AR and ENSO index are significantly negative correlated with correlation coefficient of -0.19 for zero time lags, -0.18 for 7a time ahead, and -0.20 for 27a time ahead for ENSO against AR. These correlation coefficients suggest that AR is significant but with small negative correlation with the global tropical climate. El Nino year is generally related to a lower AR in the YES for the corresponding year, 7a and 27a later. There is also a significant positive correlation with a coefficient of 0.25 for a 29a time ahead for AR against ENSO.

AR and PDO index are most significantly negative correlated with correlation coefficient of -0.30 for 28a time ahead. The correlation coefficient suggests that AR has a significant correlation with the North Pacific climate with a time of 27a later. Positive (negative) phase of PDO is related to a smaller (larger) AR of SST in the YES 27a later. There is also a very significant positive correlation with a coefficient of 0.41 for a 27a time ahead for AR against PDO.

3.6 Relationship between AM with regional and global climate

The time lagged correlation coefficients between the first EOF temporal mode of AM with TAC, PAC, EASM index, ENSO index, and PDO index are shown in the right column of Fig. 12 from top to bottom.

AR is significantly correlated with regional climate, as shown in Figs. 12f to 12h. The large and board peak in Fig. 12f shows that AM and TAC are significantly positive correlated with correlation coefficient of 0.6 for a few years time ahead for AM against TAC. This correlation coefficient suggests that AM is significantly related with the regional land air temperature anomaly, higher (lower) AM corresponds to positive (negative) TAC, and the higher AM is generally related to warm surface air temperature over China from corresponding year to a few years later.

AM and PAC are significantly negative correlation at with correlation coefficient of -0.3 for 21a and 26a ahead for PAC against AM, and 28a ahead for AM against PAC (Fig. 12g). Higher (lower) AM is related with less (more) precipitation on bi-decadal to tri-decadal time lags.

AM and EASM index are significantly negative correlated with correlation coefficient of about -0.35 for 5a time ahead and 9a and 18a time lag of EASM against AM (Fig. 12h). The correlation coefficient suggests that strong (weak) EASM is related to a lower (higher) AM in the YES for 5a later, and lower (higher) AM is related to a strong (weak) EASM 9a and 18a later.

AM and ENSO index are significantly positive correlated with small correlation coefficients of about 0.15 for 3a, 7a, 19a, and 27a time ahead and 1a, 16a and 19a time lag for ENSO against AM (Fig. 12i). These correlation coefficients suggest that El Nino year is generally related to a higher AM in the YES for 3a, 7a, 19a, or 27a later. There is also a significant negative correlation with a coefficient of 0.15 for a 29a time ahead for AM against ENSO.

AM and PDO index are significantly negative correlated with correlation coefficient of -0.20 for 10a time ahead and positively correlated with a correlation coefficient of 0.18 for 27a time ahead for PDO against AM (Fig. 12j). The correlation coefficient suggests positive (negative) phase of PDO is related to a lower (higher) AM in the YES 10a later and to higher (lower) AM in the YES 27a later. There are also significant correlation for AM ahead against PDO with a positive correlation coefficient of 0.25 and a 14a time lead, and a negative correlation coefficient of 0.25 and a 28a time lead.

4. Conclusions and discussions

The SST in the YES over the last 141 years (1870-2010) is partitioned into an AC (seasonal signal with zero mean) and an AM (inter-annual, decadal and long-term trend). The spatial and temporal variability of the AC and AM and their relationship are analyzed with pattern fitting and EOF method. The possible linkage between the identified variability with the known regional and global climate (i.e., TAC, PAC, EASM, ENSO and PDO) is also explored.

AC is represented by a mean normalized annual pattern and a time-varying AR. The mean normalized annual pattern fits well with annual and semi-annual sinusoidal signals with less than 0.04°C RMSE. The annual sinusoidal signal dominates semi-annual signal by contributing greater than 94% to AR in general; the semi-annual signal contributes to more than 10% to AR in the eastern Yellow Sea, particularly to the area south of Korean Peninsula. The annual cycle of SST reaches its highest SST from mid July in the south to early August in the north and central of YES. The mean AR increases from 6°C in the south and east of Taiwan to 24°C in the northern Bohai Sea. The STD of AR is about 0.5°C to the east of Taiwan, and increases from both sides of south and north to the western YES to a value of 1.4°C. This variance is mostly explained by the first EOF mode (69%), which has a coherent in-phase spatial pattern with maximum amplitude in the western YES.

The AM has a mean SST of 26°C in the south of YES, which decreases northward, reaches a minimum mean SST of 13°C in the northern Bohai Sea. The STD of AM has a relatively uniform spatial pattern with maximum variance of 0.7°C in the central to south-western YES. This variance is explained mostly by the first EOF mode (85%), which has a coherent in-phase spatial pattern with its maximum amplitude in the central to south-western YES.

Both AR and AM vary on inter-annual to decadal time scales, and they are significantly negative correlated with a zero and 5a time lag for AR against AM. This correlation suggest a higher (lower) AM is associated with a smaller (larger) AR for the corresponding year and 5a later. Therefore, in the years with higher (lower) AM, often have smaller (larger) AR, and consequently, experience much warmer (colder) than usual winter SST. The variability of winter SST is most significant in four seasons, and the summer SST is the least variable.

Over the last 141 years, the AM in the YES has experienced four regimes, namely, CC from 1970 to 1900, CW from 1901 to 1944, WC from 1945 to 1976, and WW from 1977 to 2010. Corresponding to these four regimes, the AC experienced a smaller, higher, normal and the smallest AR, respectively.

The SST in the YES over the last WW regime (from 1977 to 2010) increases from 0.6°C in the southeast to 2.0°C in the central of YES. During this period, the AR is significantly reduced. The combination of the warming of AM and the reduction of AR leads to a much larger SST increase in winter, i.e., the warming in winter is much more significant than in other seasons in the last WW regime, and particularly in 1998.

Both the AR and AM of SST in the YES is related to the regional and global climate. TAC is positively associated with AM and negatively associated with AR. The warmer (colder) surface air temperature over China is associated with a warmer (colder) SST in the YES, particularly in winter, through the higher (lower) AM and smaller (larger) AR.

Since the precipitation over China is primarily controlled by monsoon. Both PAC and EASM index are positively correlated with AR, and negatively correlated with AM. Both inter-decadal time lagged and leaded significant correlations between AM and PAC suggest that AM and PAC might have some interaction on inter-decadal time scales. Both inter-annual to inter-decadal time lagged and leaded significant correlation between AM and EASM index suggest that AM and EASM might have some interaction on these time scales.

Both the small coefficient between AM and AR with ENSO and PDO indexes mean that AM and AR are definitely related to the variability of the large scale Tropic Ocean and North Pacific Ocean climate, but the contribution from the global climate to the variability of AM and AR in the YES is only about 15-20%. The relatively larger correlation coefficient of between AM and AR with TAC, PAC and EASM index mean that regional climate is more closely related to the variability of SST in the YES.

5. Acknowledgment

HadISST1 data is provided by the Met Office Hadley Centre, UK, dataset is downloaded from http://www.metoffice.gov.uk/hadobs/hadisst/data/download.html. EASM index is provided by Jianping Li at State Key Laboratory of Numerical Modeling for Atmospheric Sciences and Geophysical Fluid Dynamics, Institute of Atmospheric Physics, Chinese Academy of Sciences, and is downloaded from http://web.lasg.ac.cn/ staff/ ljp/ data-monsoon/ EASMI.htm. ENSO index is provided by JMA and is downloaded from http://coaps.fsu.edu/pub/JMA_SST_Index/. PDO index is provided by Nathan Mantua at Joint Institute for the Study of the Atmosphere and Ocean (JISAO), Washington University, dataset is downloaded from http://jisao.washington.edu/ pdo/PDO.latest. This research was supported by the National Basic Research Program of China under Grant No. 2006CB400603 and 2011CB409803, the Zhejiang Provincial Natural Science Foundation of China under Grant No. R504040, the Natural Science Foundation of China under Grant No. 41176021, and the China 908-Project under Grant No. 908-ZC-II-05 and 908-ZC-I-13.

6. References

Chen, D.; Liu, W.T.; Tang, W. & Wang, Z. (2003). Air-sea interaction at an oceanic front: Implications for frontogenesis and primary production, *Geophysical Research Letter*, Vol. 30, No. 14, 1745, doi:10.1029/2003GL017536

Ding, Y. & Ren, Y. (Eds). (2008). *Introduction to climate change in China*, China Meteorological Press, ISBN 978-7-5029-4364-6, Beijing. (In Chinese)

Emery, W.J. & Thomson, R.E. (Eds). (2001). *Data analysis methods in physical oceanography*, Second and revised edition, Elsevier Science B.V., ISBN 0-444-50757-4, Amsterdam, The Netherlands.

Hahn, S.D. (1994). SST warming of Korean coastal waters during 1881-1900, KODC Newsletter 24, pp. 29-37.

Huang, D.; Zhao, J. & Su, J. (2003). Practical implementation of Hilbert-Huang Transform algorithm. *Acta Oceanologica Sinica*, Vol. 22, No. 1, pp. 1-14.

Huang, N.E.; Shen, Z.; Long, S.R.; Wu, M.C.; Shih, H.H.; Zheng, Q.; Yen, N.-C.; Tung, C.C. & Liu, H.H. (1998). The empirical mode decomposition and the Hilbert spectrum for nonlinear and non-stationary time series analysis. *Proceedings of Royal Society of London A*, Vol. 454, No. 1971, pp. 903-995.

Huang, N.E. & Wu, Z. (2008). A review on Hilbert-Huang transform: Method and its applications to geophysical studies. *Review of Geophysics*, Vol. 46, RG2006, doi:10.1029/2007RG000228.

Kang, I. & Jeong, Y. (1996). Association of interannual variations of temperature and precipitation in Seoul with principal modes of Pacific SST, *Journal of the Korean Meteorological Society*, Vol. 32, pp. 339–345

Jones, P.D. & Moberg, A. (2003). Hemispheric and Large-Scale Surface Air Temperature Variations: An Extensive Revision and an Update to 2001. *Journal of Climate*, Vol. 16, No. 2, pp. 206-223.

Li, J. & Zeng, Q. (2003). A new monsoon index and the geographical distribution of the global monsoons. *Advance in Atmospheric Sciences*, Vol. 20, No. 2, pp. 299-302.

Lin, C.; Su, J.; Xu, B. & Tang, Q. (2001). Long-term variations of temperature and salinity of the Bohai Sea and their influence on its ecosystem. *Progress in Oceanography*, Vol. 49, pp. 7–19.

Lin, C.; Ning, X.; Su, J.; Lin, Y. & Xu, B. (2005). Environmental changes and the responses of the ecosystems of the Yellow Sea during 1976–2000. *Journal of Marine Systems*, Vol. 55, pp. 223–234.

Mantua, N.J.; Hare, S.R.; Zhang, Y.; Wallace, J.M. & Francis, R.C. (1997). A Pacific interdecadal climate oscillation with impacts on salmon production. *Bulletin of the American Meteorological Society*, Vol. 78, No. 6, pp. 1069-1079

Meyers, S.D., O'Brien, J.J. & Thelin, E. (1999): Reconstruction of monthly SST in the Tropical Pacific Ocean during 1868-1993 using adaptive climate basis functions. *J. Climate*, Vol. 127, No. 7, pp. 1599-1612

Rayner, N.A.; Parker, D.E.; Horton, E.B.; Folland, C.K.; Alexander, L.V.; Rowell, D.P.; Kent, E.C. & Kaplan, A. (2003). Global analyses of sea surface temperature, sea ice, and night marine air temperature since the late nineteenth century. *Journal of Geophysical Research*, Vol. 108, No. D14, 4407, doi:10.1029/2002JD002670

Tang, G. & Ren, G. (2005). Reanalysis of surface air temperature change of the last 100 Years over china, *Climatic and Environmental Research*, Vol. 10, No. 4, pp. 791-798. (In Chinese)

Tao, S. & Zhang, Q. (1998). Response of the East Asian winter and summer monsoon to ENSO events, *Scientia Atmosphetica Sinica*, Vol. 22, pp. 399–407. (In Chinese)

Wang, B.; Wu, R. & Fu, X. (2000). Pacific–East Asian Teleconnection: How Does ENSO Affect East Asian Climate? *Journal of Climate*, Vol. 13, No. 9, pp. 1517–1536

Webster, P.J.; Magana, V.O.; Palmer, T. N.; Tomas, T. A.; Yanai, M. & Yasunari, T. (1998). Monsoons: Processes, predictability, and prospects for prediction, *Journal of Geophysical Research*, Vol. 103, No. C7, pp. 14451–14510

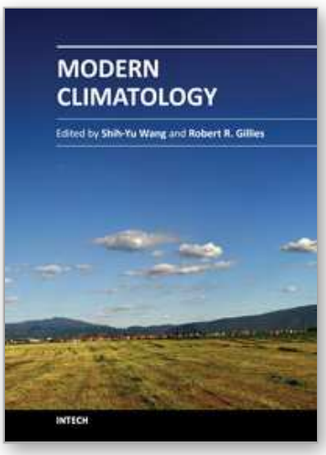
Xie, S.; Hafner, J.; Tanimoto, Y.; Liu, W.T.; Tokinaga, H. & Xu, H. (2002). Bathymetric effect on the winter sea surface temperature and climate of the Yellow and East China Seas, *Geophysical Research Letter*, Vol. 29, No. 24, 2228, doi:10.1029/2002GL015884

Zhang X.Z.; Qiu, Y.F. & Wu, X.Y. (2005). The Long-term change for sea surface temperature in the last 100 Years in the offshore sea of China. *Climatic and Environmental Research*, Vol. 10, No. 4, pp. 709-807. (In Chinese with English abstract)

Zhang, Y.; Wallace, J.M. & Battisti, D.S. (1997). ENSO-like interdecadal variability: 1900-93. *Journal of Climate*, Vol. 10, No. 5, pp. 1004-1020

IntechOpen

IntechOpen



Modern Climatology

Edited by Dr Shih-Yu Wang

ISBN 978-953-51-0095-9
Hard cover, 398 pages
Publisher InTech
Published online 09, March, 2012
Published in print edition March, 2012

Climatology, the study of climate, is no longer regarded as a single discipline that treats climate as something that fluctuates only within the unchanging boundaries described by historical statistics. The field has recognized that climate is something that changes continually under the influence of physical and biological forces and so, cannot be understood in isolation but rather, is one that includes diverse scientific disciplines that play their role in understanding a highly complex coupled "whole system" that is the earth's climate. The modern era of climatology is echoed in this book. On the one hand it offers a broad synoptic perspective but also considers the regional standpoint, as it is this that affects what people need from climatology. Aspects on the topic of climate change - what is often considered a contradiction in terms - is also addressed. It is all too evident these days that what recent work in climatology has revealed carries profound implications for economic and social policy; it is with these in mind that the final chapters consider acumens as to the application of what has been learned to date.

How to reference

In order to correctly reference this scholarly work, feel free to copy and paste the following:

Daji Huang, Xiaobo Ni, Qisheng Tang, Xiaohua Zhu and Dongfeng Xu (2012). Spatial and Temporal Variability of Sea Surface Temperature in the Yellow Sea and East China Sea over the Past 141 Years, Modern Climatology, Dr Shih-Yu Wang (Ed.), ISBN: 978-953-51-0095-9, InTech, Available from: http://www.intechopen.com/books/modern-climatology/spatial-and-temporal-variability-of-sea-surface-temperature-in-the-yellow-sea-and-east-china-sea-ove

INTECH
open science | open minds

InTech Europe
University Campus STeP Ri
Slavka Krautzeka 83/A
51000 Rijeka, Croatia
Phone: +385 (51) 770 447
Fax: +385 (51) 686 166
www.intechopen.com

InTech China
Unit 405, Office Block, Hotel Equatorial Shanghai
No.65, Yan An Road (West), Shanghai, 200040, China
中国上海市延安西路65号上海国际贵都大饭店办公楼405单元
Phone: +86-21-62489820
Fax: +86-21-62489821

© 2012 The Author(s). Licensee IntechOpen. This is an open access article distributed under the terms of the Creative Commons Attribution 3.0 License, which permits unrestricted use, distribution, and reproduction in any medium, provided the original work is properly cited.

IntechOpen

IntechOpen